Available online at www.sciencedirect.com
ScienceDirect
Journal of Solid State Chemistry 179 (2006) 3059–3064
JOURNAL OF SOLID STATE CHEMISTRY
www.elsevier.com/locate/jssc

Synthesis and structural characterization of two polymorphs of Fe(2,2′-bpy)(HPO_4)(H_2PO_4)

Wen-Jung Chang[a], Yau-Chen Jiang[b], Sue-Lein Wang[b], Kwang-Hwa Lii[a,c,*]

[a]*Department of Chemistry, National Central University, Chungli, Taiwan 320, ROC*
[b]*Department of Chemistry, National Tsing Hua University, Hsinchu, Taiwan 300, ROC*
[c]*Institute of Chemistry, Academia Sinica, Taipei, Taiwan 115, ROC*

Received 30 December 2005; received in revised form 12 May 2006; accepted 28 May 2006
Available online 7 June 2006

Abstract

Two polymorphs of an organic–inorganic hybrid compound, Fe(2,2′-bpy)(HPO_4)(H_2PO_4) (**1** and **2**) (2,2′-bpy = 2,2′-bipyridine), have been synthesized by hydrothermal methods and structurally characterized by single-crystal X-ray diffraction, thermogravimetric analysis, and magnetic susceptibility. Crystal data are as follows: Polymorph **1**, monoclinic, space group $P2_1/n$ (No. 14), $a = 10.904(2)$ Å, $b = 6.423(1)$ Å, $c = 19.314(3)$ Å, $\beta = 101.161(3)^\circ$, and $Z = 4$; Polymorph **2**, monoclinic, space group $P2_1/c$ (No. 14), $a = 11.014(1)$ Å, $b = 15.872(2)$ Å, $c = 8.444(1)$ Å, $\beta = 109.085(3)^\circ$, and $Z = 4$. Polymorph **1** adopts a chain structure in which each iron atom is coordinated by two nitrogen atoms from 2,2′-bpy ligand and four phosphate oxygen atoms. These infinite chains are extended into a 3-D supramolecular array via π–π stacking interactions of the lateral 2,2′-bpy ligands. The structure of polymorph **2** consists of the same building units, namely FeO_4N_2 octahedron, HPO_4 and H_2PO_4 tetrahedra, and 2,2′-bpy ligand, which are linked through their vertices forming an undulated sheetlike structure with 4,12 network. Adjacent layers are extended into a 3-D array via π–π stacking interactions of the aromatic groups. Magnetic susceptibility measurement results confirm that the iron atoms in both compounds are present in the +3 oxidation state.

Keywords: Phosphate; Iron; Polymorph; Crystal structure; Hydrothermal synthesis

1. Introduction

Recently, many research activities have focused on the synthesis of open-framework metal phosphates with organic ligands. The underlying idea is to combine the robustness of inorganic phosphate frameworks with the versatility and chemical flexibility of organic ligands. Such organic–inorganic hybrid compounds can also combine characteristics of each component to produce novel structural types. It has been established that oxalate readily substitutes for phosphate in the skeleton of inorganic phosphates forming a large number of oxalate–phosphate hybrid compounds [1]. Another class of organic–inorganic hybrid compounds is based on 4,4′-bipyridine and phosphate, in which the metal cations are coordinated by both types of ligands [2]. In these structures, the 4,4′-bpy unit can act as a diprotonated counter cation, a monoprotonated pendant ligand or as a neutral bridging ligand. About half of the reported structures in this system consist of metal phosphate layers pillared by 4,4′-bpy ligands. This structure type exhibits the characteristic pattern of alternating organic–inorganic domains often observed in metal organophosphonate phases. Recently, we were interested in using 2,2′-bipyridine (2,2′-bpy) or 1,10-phenanthroline (phen) to synthesize new organic–inorganic hybrid compounds, and have isolated the first fluorinated metal phosphates with bpy ligand, namely Fe_2F_2(2,2′-bpy)(HPO_4)$_2$(H_2O) and the gallium analog [3]. We have also synthesized two new compounds in the Ga/phen/PO_4 system with chain structures and applied ^{2}H MAS NMR spectroscopy to study the very short hydrogen bond [4].

*Corresponding author. The Faculty of Science, The Department of Chemistry, The National Central University, Number 300, Junda Road, Jhongli city, Taoyuan county 32054, Taiwan, ROC. Fax: +886 3 422 7664.
E-mail address: liikh@cc.ncu.edu.tw (K.-H. Lii).

0022-4596/$ - see front matter © 2006 Elsevier Inc. All rights reserved.
doi:10.1016/j.jssc.2006.05.035

A good number of metal phosphates with bpy and phen ligands have been reported by other researchers [5]. Herein, we describe the synthesis and structural characterization of two new polymorphs in this family, Fe(2,2′-bpy)$(HPO_4)(H_2PO_4)$ (denoted as **1** and **2**). This is the first example introducing the polymorphs of the metal phosphates incorporating 2,2′-bpy ligands.

2. Experimental section

2.1. Synthesis and initial characterization

The hydrothermal reactions were carried out in Teflon-lined stainless steel Parr acid digestion bombs under autogeneous pressure. All chemicals were purchased from Aldrich. A reaction mixture of $FeCl_3 \cdot 6H_2O$ (1 mmol), 2,2′-bipyridine (5 mmol), $(NH_4)H_2PO_4$ (4 mmol), H_3PO_4 (2 mmol), TEABr (tetraethylammonium bromide, 2 mmol), ethylene glycol (3 mL) and H_2O (9 mL) was heated at 165 °C for 3 days followed by slow cooling to room temperature at 10 °C/h. The pH values of the solution before and after the hydrothermal reaction were 4.6 and 3.5, respectively. The solid product was filtered off, washed with water, rinsed with ethanol and dried at room temperature to give yellow–green prismatic crystals of **1** with 78% yield based on iron. The X-ray powder pattern of the bulk product was in good agreement with the calculated pattern based on the atomic coordinates derived from single-crystal X-ray diffraction (Fig. S1(a)) thus suggesting it to be monophasic. Powder X-ray data were collected on a Shimadzu XRD-6000 powder diffractometer with Cu$K\alpha$ radiation equipped with a scintillation detector. Data were collected in the range $5^\circ < 2\theta < 50^\circ$ using $\theta-2\theta$ mode in a Bragg–Brentano geometry. Elemental analysis confirmed its stoichiometry. *Anal. Found*: C, 29.65; H, 2.74; N, 6.87%. *Calc.*: C, 29.08; H, 2.66; N, 6.92% for **1**. We have also carried out the same reactions without TEABr in the reaction mixture, but unable to get the polymorph **1**.

Yellow–green columnar crystals of compound **2** were obtained with a yield of 90% by heating $FeCl_3 \cdot 6H_2O$ (1 mmol), 2,2′-bipyridine (2 mmol), $(NH_4)H_2PO_4$ (3 mmol), H_3PO_4 (2 mmol), ethylene glycol (3 mL) and H_2O (9 mL) under the same reaction conditions as those for **1**. The pH values of the solution before and after the hydrothermal reaction were 3.7 and 3.3, respectively. The product was mononphasic as indicated by powder X-ray diffraction (Fig. S1(b)). Elemental analysis confirmed its stoichiometry. *Anal. Found*: C, 29.07; H, 2.88; N, 6.61% *Calc.*: C, 29.08; H, 2.66; N, 6.92% for **2**.

Thermogravimetric analysis was performed on a Perkin-Elmer TGA7 thermal analyzer; the sample was heated in flowing oxygen from 50 to 350 °C at 10 °C/min followed by subsequent change to 5 °C/min from 350 to 900 °C. The change to a lower heating rate can reduce the time lag between furnace and specimen temperatures so that the specimen is fully oxidized in the temperature range. DSC measurements of both **1** and **2** between room temperature and 300 °C did not reveal a phase change.

2.2. Single-crystal X-ray diffraction

Yellow–green crystals of dimension $0.25 \times 0.23 \times 0.06\,mm^3$ and $0.15 \times 0.06 \times 0.06\,mm^3$ for **1** and **2**, respectively, were selected for indexing and intensity data collection on a Siemens Smart-CCD diffractometer equipped with a normal focus, 3 kW sealed tube X-ray source at room temperature. Empirical absorption corrections based on symmetry equivalents were performed by using the SADABS program for the Siemens area detector ($T_{min/max} = 0.745/0.899$ for **1**; 0.842/0.956 for **2**) [6]. The two structures were solved by direct methods and refined by full-matrix least-squares on F^2. The iron and phosphorus atoms were first located, and the carbon, nitrogen and oxygen atoms were found in subsequent difference Fourier maps. Bond-valence calculations indicate that O(1), O(6) and O(8) in **1** and O(1), O(5) and O(6) in **2** are hydroxyl oxygen atoms [7]. The hydrogen atoms, which are bonded to carbon atoms, were positioned geometrically and refined using a riding model with fixed isotropic thermal parameters. The final cycles of least-squares refinement included atomic coordinates and anisotropic thermal parameters for all non-hydrogen atoms. The reliability factors converged to $R_1 = 0.0505$, $wR_2 = 0.1319$, and $S = 1.091$ for **1** and $R_1 = 0.0643$, $wR_2 = 0.1130$, and $S = 1.050$ for **2**. All calculations were performed using SHELXTL Version 5.1 software package [8]. The crystallographic data are given in Table 1 and bond distances in Table 2.

Table 1
The crystallographic data for Fe(2,2′-bpy)$(HPO_4)(H_2PO_4)$ (**1** and **2**)

	1	**2**
Chemical formula	$C_{10}H_{11}N_2O_8P_2Fe$	$C_{10}H_{11}N_2O_8P_2Fe$
a/Å	10.904(2)	11.014(1)
b/Å	6.423(1)	15.872(2)
c/Å	19.314(3)	8.444(1)
β/deg	101.161(3)	109.085(3)
V/Å^3	1327.0(4)	1395.1(3)
Z	4	4
Formula weight	405.00	405.00
Space group	$P2_1/n$ (No. 14)	$P2_1/c$ (No. 14)
T, K	296	296
λ(Mo$K\alpha$), Å	0.71073	0.71073
D_{calc}, g/cm^3	2.027	1.928
μ(Mo$K\alpha$), cm^{-1}	14.3	13.6
Number of reflections collected	8058	8815
Unique data ($I > 2\sigma(I)$)	1926	1950
Number of least-squares parameters	209	208
$R1$[a]	0.0505	0.0643
wR_2[b]	0.1319	0.1130

[a] $R_1 = \Sigma||F_o|-|F_c||/\Sigma|F_o|$.

[b] $wR_2 = [\Sigma w(F_o^2-F_c^2)^2/\Sigma w(F_{o2})^2]^{1/2}$, $w = 1/[\sigma^2(F_o^2)+(aP)^2+bP]$, $P = [\text{Max}(F_o^2,0)+2(F_c)^2]/3$, where $a = 0.0587$ and $b = 0$ for **1** and $a = 0.0218$ and $b = 2.64$ for **2**.

Table 2
Bond lengths (Å) for Fe(2,2′-bpy)(HPO_4)(H_2PO_4) (**1** and **2**)[a]

Compound **1**		Compound **2**	
Fe(1)–O(7)	1.928(3)	Fe(1)–O(7)	2.008(4)
Fe(1)–O(2)	1.930(3)	Fe(1)–O(2)	1.916(3)
Fe(1)–O(4)	1.975(3)	Fe(1)–O(4)	1.971(4)
Fe(1)–O(3)	2.050(3)	Fe(1)–O(8)	1.926(3)
Fe(1)–N(1)	2.154(4)	Fe(1)–N(1)	2.153(4)
Fe(1)–N(2)	2.184(4)	Fe(1)–N(2)	2.164(4)
P(1)–O(1)	1.573(3)	P(1)–O(1)	1.572(4)
P(1)–O(2)	1.521(3)	P(1)–O(2)	1.519(4)
P(1)–O(3)	1.541(3)	P(1)–O(3)	1.531(4)
P(1)–O(4)	1.515(3)	P(1)–O(4)	1.497(4)
P(2)–O(5)	1.504(3)	P(2)–O(5)	1.548(4)
P(2)–O(6)	1.547(3)	P(2)–O(6)	1.550(4)
P(2)–O(7)	1.508(3)	P(2)–O(7)	1.488(4)
P(2)–O(8)	1.564(3)	P(2)–O(8)	1.505(3)
O(1)–H(O1)	0.908	O(1)–H(O1)	0.950
O(6)–H(O6)	0.986	O(5)–H(O5)	1.000
O(8)–H(O8)	0.968	O(6)–H(O6)	1.141
N(1)–C(1)	1.350(6)	N(1)–C(1)	1.314(7)
N(1)–C(5)	1.356(6)	N(1)–C(5)	1.368(7)
N(2)–C(6)	1.343(6)	N(2)–C(6)	1.342(7)
N(2)–C(10)	1.335(6)	N(2)–C(10)	1.323(7)
C(1)–C(2)	1.370(7)	C(1)–C(2)	1.378(8)
C(2)–C(3)	1.364(8)	C(2)–C(3)	1.37(1)
C(3)–C(4)	1.395(7)	C(3)–C(4)	1.37(1)
C(4)–C(5)	1.386(6)	C(4)–C(5)	1.381(8)
C(5)–C(6)	1.492(6)	C(5)–C(6)	1.452(9)
C(6)–C(7)	1.379(6)	C(6)–C(7)	1.402(8)
C(7)–C(8)	1.382(7)	C(7)–C(8)	1.36(1)
C(8)–C(9)	1.368(8)	C(8)–C(9)	1.35(1)
C(9)–C(10)	1.385(7)	C(9)–C(10)	1.386(9)

[a]The C–H bond lengths are 0.93 Å.

2.3. Magnetic susceptibility measurements

Variable-temperature magnetic susceptibility $\chi(T)$ data were obtained on suitable amount of polycrystalline samples of **1** and **2** from 2 to 300 K in a magnetic field of 5000 G after zero-field cooling using a SQUID magnetometer. Correction for diamagnetism was made according to Kahn [9].

3. Results and discussion

3.1. Crystal structures

3.1.1. Fe(2,2′-bpy)(HPO_4)(H_2PO_4) (1)

Polymorph **1** crystallizes in the monoclinic space group $P2_1/n$ with unit cell content of four formula units. All atoms are at general positions. Fig. 1(a) shows the coordination environment of Fe(1). The Fe atom is octahedrally coordinated by one bidentate 2,2′-bpy and four phosphate ligands. Compound **1** has a chain structure. The fundamental building unit includes a FeO_4N_2 octahedron, 3 HPO_4 tetrahedra, 1 H_2PO_4 tetrahedron and a 2,2′-bpy ligand. The connectivity between these units is made by HP(1)O_4 group that joins neighboring three iron octahedra to form infinite chains parallel to the [010] direction (Fig. 2). Each $H_2P(2)O_4$ group has one oxygen bridging to FeO_4N_2 and extends away from the chain as a pendant group, which accounts for the relatively larger thermal parameters of the atoms in the group. Of the remaining three P(2)–O bonds, the longer two constitutes the P–OH groups, while the third is a terminal P–O bond possessing multiple bond character (P(2)–O(5) = 1.504 Å). The infinite chains are held in position by hydrogen bonds between the pendant H_2PO_4 groups and attractive intermolecular aromatic interaction between 2,2′-bpy ligands into a 3-D supramolecular array (Fig. 3). Adjacent 2,2′-bpy ligands are parallel and separated around 3.7 Å, which indicates significant π–π interaction.

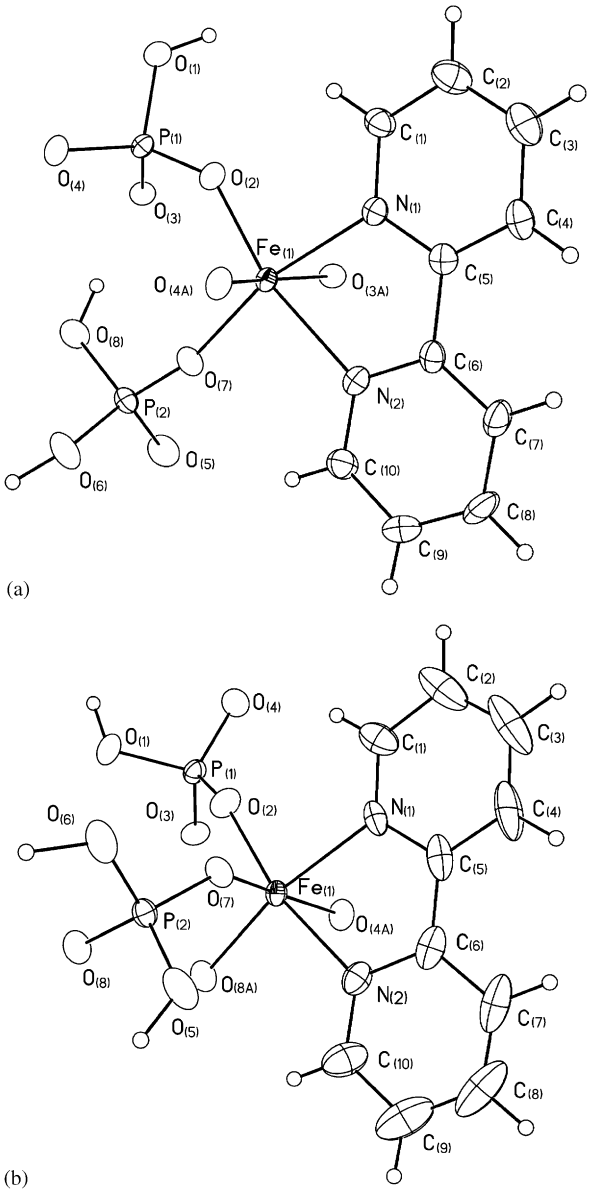

Fig. 1. The coordination environment of Fe atom in the structure of **1** (a) and **2** (b). Thermal ellipsoids are shown at 50% probability. Small open circles represent H atoms.

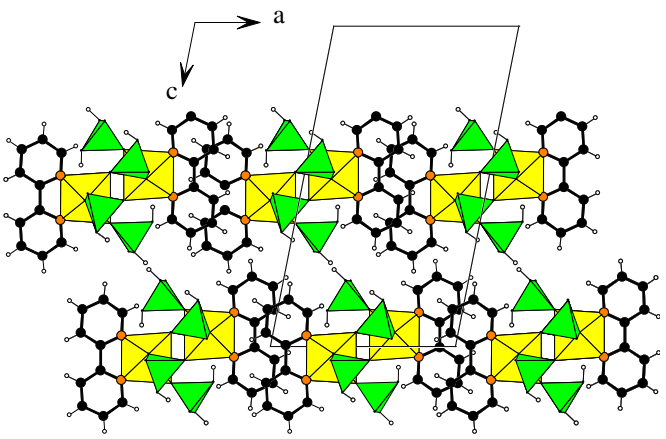

Fig. 2. Projection of the structure of **1** onto the *ac*-plane. The yellow and green polyhedra are iron octahedra and phosphate tetrahedra, respectively. Key: black circles, C atoms; orange circles, N atoms; small open circles, H atoms.

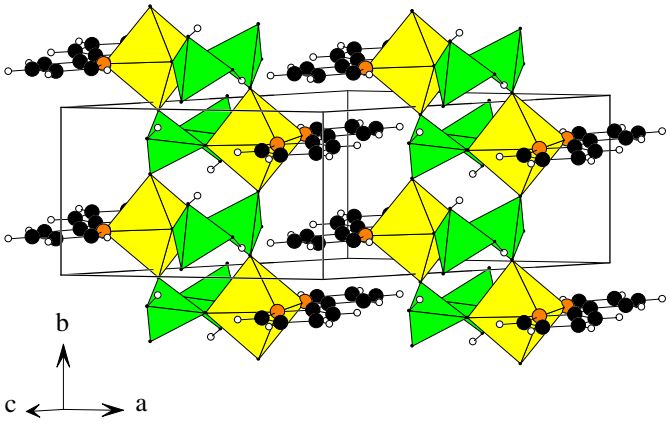

Fig. 3. Sections of two infinite chains in **1** showing π–π stacking interactions between neighboring 2,2′-bpy ligands from adjacent chains.

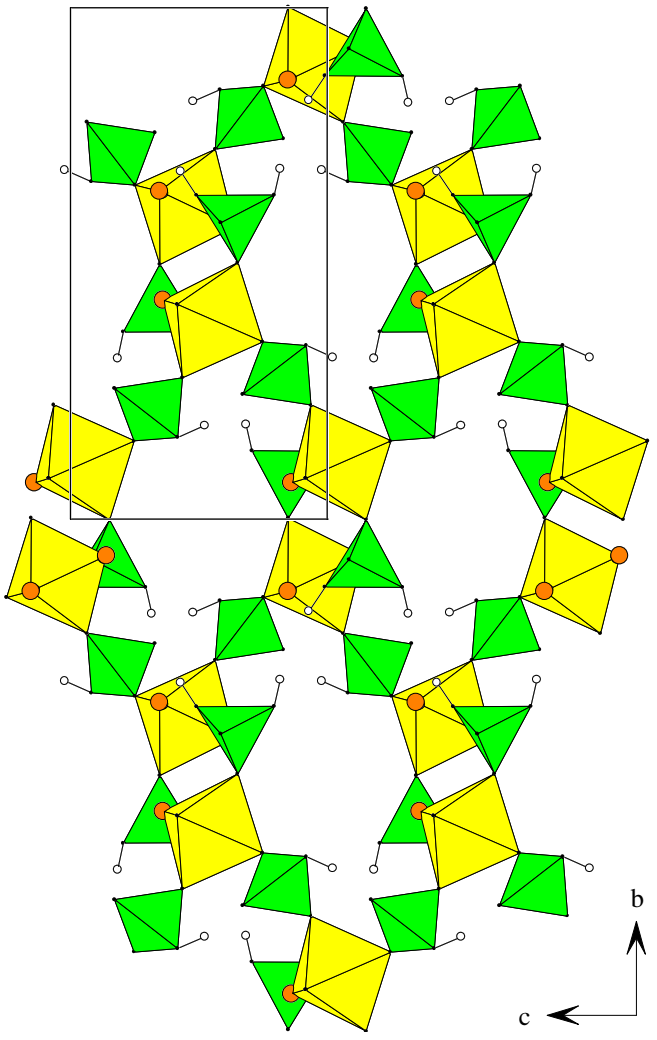

Fig. 4. Section of a layer in **2**. The yellow and green polyhedra are gallium octahedra and phosphate tetrahedra, respectively. Key: black circles, C atoms; orange circles, N atoms; small open circles, H atoms.

3.1.2. *Fe(2,2′-bpy)(HPO$_4$)(H$_2$PO$_4$) (2)*

Polymorph **2** crystallizes in the monoclinic space group $P2_1/c$ with unit cell content of four formula units. Fig. 1(b) shows the coordination environment of Fe(1). The Fe atom is octahedrally coordinated by one bidentate 2,2′-bpy, two H_2PO_4, and two HPO_4 ligands. Each of the two independent P atoms makes two P–O–Fe linkages. Polymorph **2** has a layer structure. The fundamental building units include one FeO_4N_2 octahedron, 2 HPO_4 tetrahedra, 2 H_2PO_4 tetrahedra, and one 2,2′-bpy ligand. These units are connected to form 4- and 12-membered rings within a layer, as shown in Fig. 4. Each iron phosphate layer is joined with 2,2′-bpy ligands projecting above and below into the interlamellar region (Fig. 5). Neighboring 2,2′-bpy ligands from two adjacent layers have a structure of zig-zag stacking and separated around 3.4 Å, indicating strong attractive intermolecular aromatic interaction. Thus, iron phosphate layers are extended into a 3-D supramolecular array via π–π stacking interactions of the 2,2′-bpy ligands.

Fig. 6 is a schematic representation of a chain in **1** and a layer in **2**. The structure of **1** consists of four-membered rings formed by two $Fe(1)O_4N_2$ octahedra and two $HP(1)O_4$ tetrahedra via corner-sharing and there is $H_2P(2)O_4$ attached to each metal atom as a pendant group. An analogous chain has also been observed in several metal phosphates with phen ligand, namely $[Ga(phen)(HPO_4)(H_2PO_4)]\cdot 1.5H_2O$ [4], $[Fe(phen)(HPO_4)(H_2PO_4)]\cdot 0.5H_2O$ [5i], and $[Cd(phen)(H_2PO_4)_2]\cdot H_2O$.[5j] The 2-D layers in **2** consists of 4- and 12-membered rings. Each 4-membered ring is formed of two $Fe(1)O_4N_2$ octahedra and two $H_2P(2)O_4$ tetrahedra. The 4-membered rings are connected by $HP(1)O_4$ groups such that layers with 12-membered rings are formed. Compound **2** is isostructural with Ga(2,2′-bpy)(HPO$_4$)(H$_2$PO$_4$) [5h].

3.1.3. *Thermogravimetric analysis*

As shown in Fig. 7, the TGA curve for **1** (dashed line) shows a broad weight loss in several steps, which commences gradually at ca. 250 °C and is complete at 750 °C. The observed weight loss in the first step between

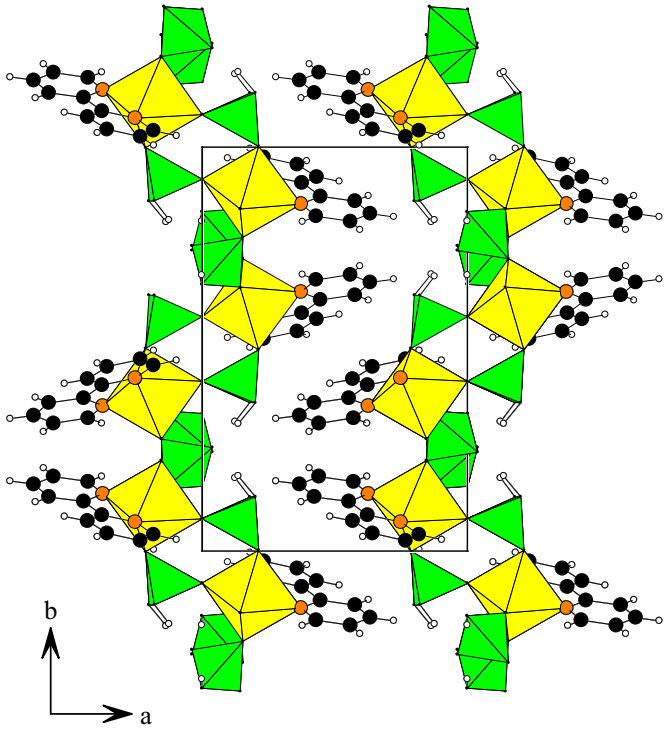

Fig. 5. Structure of **2** viewed along the *c*-axis.

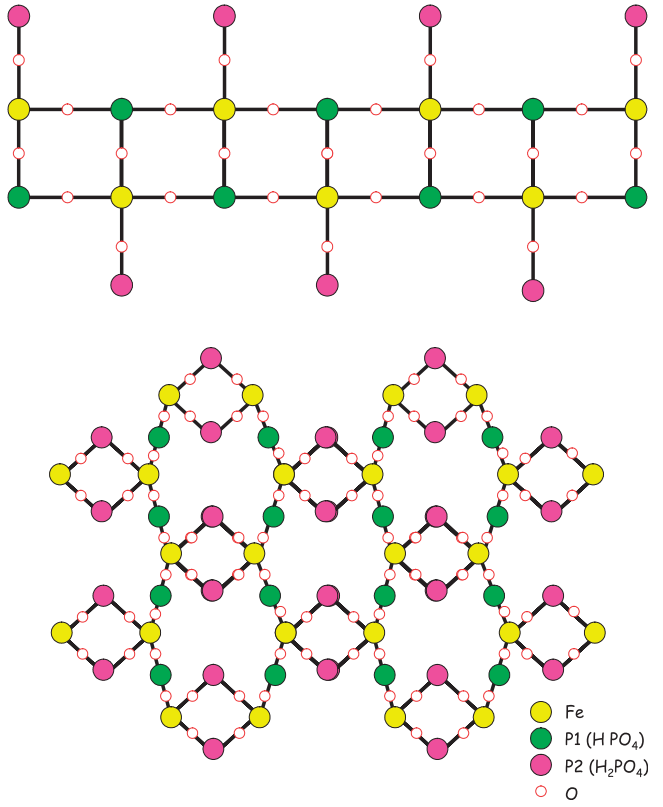

Fig. 6. Schematic representation of a 1-D chain in **1** (top) and 2-D layer in **2** (bottom). The 2, 2′-bpy ligands are not shown.

250 and 400 °C was 6.32% which is close to that calculated for the loss of 1.5 H_2O molecules per formula unit (6.67%) due to the condensation of hydrogen phosphate groups. The final decomposition products are $Fe_4(P_2O_7)_3$ (JCPDS: 36-0318) and $Fe(PO_3)_3$ (JCPDS: 38-109), as indicated from powder X-ray diffraction. The total weight loss between 40 and 900 °C is 45.79% which is close to the calculated value of 45.23% according to the following equation:

$$6Fe(2,2')(HPO_4)(H_2PO_4) \rightarrow Fe_4(P_2O_7)_3 + 2Fe(PO_3)_3 + 6\ C_{10}H_8N_2 + 9H_2O.$$

The XRD pattern of a sample that has been heated at 200 °C in an oven for 8 h shows that the structure of **1** is maintained.

The TGA curve for **2** (Fig. 7, solid line) shows a broad weight loss in several overlapping steps, which commences at about 375 °C and is complete at 800 °C. The observed total weight loss and the final decomposition products are the same as those for **1**. The condensation of hydrogen phosphate groups in **2** occurs at a much higher temperature. The XRD pattern of a sample that has been heated at 350 °C for 8 h shows that the structure of **2** is decomposed.

3.1.4. Magnetic susceptibility

The temperature dependence of $\chi_M T$ and $1/\chi_M$ curves, where χ_M is the molar magnetic susceptibility, are shown in Fig. S2. The $\chi_M T$ value decreases with decreasing temperature, indicating that the main interactions between Fe atoms in both compounds are antiferromagnetic (AF).

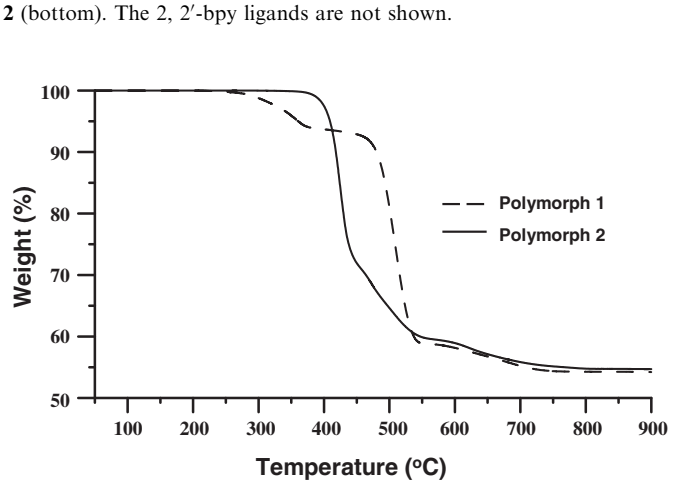

Fig. 7. Thermogravimetric analysis of **1** (dashed line) and **2** (solid line) in flowing oxygen.

The effective magnetic moment at 300 K is 2.83 $(\chi_M T)^{1/2} = 5.73\,\mu_B$/Fe for **1** and $5.67\,\mu_B$/Fe for **2**, which are in agreement with the observed magnetic moment of $5.75\,\mu_B$/Fe for $Fe^{III}_2F_2(2,2'\text{-bpy})(HPO_4)_2(H_2O)$ [3]. The magnetic susceptibilities above about 25 K follow the Curie–Weiss law with negative values of the Weiss constant. The data from 25 to 300 K were described by the equation $\chi M = C/(T-\theta)$, where $C = 4.50\,cm^3\,K/mol$ and $\theta = -29.8$ K for **1** and $C = 4.54\,cm^3\,K/mol$ and $\theta = -30.0$ K for **2**. From the equation $C = N\mu_{eff}/3k_B$, one obtains an effective magnetic moment μ_{eff} per iron ion of

6.00 μ_B for **1** and 6.03 μ_B for **2**, which are consistent with the value of 5.92 μ_B/Fe expected for spin-only and non-interacting Fe^{3+} ions. The χ_M versus T curves show peaks at 16 K for both **1** and **2**.

An important point to be noted is that the use of TEABr in the synthesis process led to the structure of **1**, whereas attempts to synthesize the compound without TEABr resulted in structure of **2**. It is likely that TEABr could have played a subtle role during the assembly of the secondary building units into a chain structure. Such example is also seen in Ga/phen/PO_4 system [4] and $[Ga_5(OH)_2(C_{10}H_9N_2)(C_2O_4)(PO_4)_4]\cdot 2H_2O$ [10], when $LiBO_2$ or 2-methylpiperazine is added, new structures can be obtained. Compound **2** is isostructural with Ga(2,2′-bpy)(HPO_4)(H_2PO_4). Attempts to synthesize the gallium analog of **1** were unsuccessful although TEABr was added in the reaction mixture.

In summary, two polymorphs of an organic–inorganic hybrid compound have been synthesized by hydrothermal reactions. The synthesis has many parameters and a subtle change in the reaction conditions can greatly affect the course of the reactions. It appears that the addition of tetraethylammonium bromide to the reaction mixture is important to the formation of **1**. Both polymorphs consist of similar secondary building units which are extended into 3-D supramolecular arrays via hydrogen bonds and π–π stacking interactions of 2,2′-bpy ligands. Polymorph **1** displays a chain structure, whereas **2** adopts a layer structure. To our knowledge, it is the first example to describe the polymorphs of a metal phosphate incorporating organic ligands. The M/bpy (or phen)/PO_4 phases have a rich structural chemistry. Further research on this interesting system is in progress.

Supplementary materials

CIF file for **1** and **2** has been deposited with the Cambridge Crystallographic Data center as Supplementary publication no. CCDC-294094 & 294095. Other supplementary data include magnetic susceptibility measurement results and X-ray powder patterns.

Acknowledgments

The authors thank the National Science Council of Taiwan for financial support.

Appendix A. Supplementary materials

The online version of this article contains additional supplementary data. Please visit doi:10.1016/j.jssc.2006.05.035.

References

[1] (a) H.-M. Lin, K.-H. Lii, Y.-C. Jiang, S.-L. Wang, Chem. Mater. 11 (1999) 519;
(b) L.-C. Hung, H.-M. Kao, K.-H. Lii, Chem. Mater. 12 (2000) 2411;
(c) Y.-C. Jiang, S.-L. Wang, S.-F. Lee, K.-H. Lii, Inorg. Chem. 42 (2003) 6154;
(d) Z.A.D. Lethbridge, P. Lightfoot, J. Solid State Chem. 143 (1999) 58;
(e) Z.A.D. Lethbridge, S.K. Tiwary, A. Harrison, P. Lightfoot, J. Chem. Soc. Dalton Trans. (2001) 1904;
(f) S. Natarajan, J. Solid State Chem. 139 (1998) 200;
(g) A. Choudhury, S. Natarajan, C.N.R. Rao, J. Solid State Chem. 146 (1999) 538;
(h) A. Choudhury, S. Natarajan, C.N.R. Rao, Chem.-Eur. J. 6 (2000) 1168;
(i) J. Do, R.P. Bontchev, A.J. Jacobson, Chem. Mater. 13 (2001) 2601;
(j) C.T.S. Choi, E.V. Anokhina, C.S. Day, Y. Zhao, F. Taulelle, C. Huguenard, Z. Gan, A. Lachgar, Chem. Mater. 14 (2002) 4096.
[2] (a) K.-H. Lii, Y.-F. Huang, Inorg. Chem. 38 (1999) 1348;
(b) C.-Y. Chen, F.-R. Lo, H.-M. Kao, K.-H. Lii, Chem. Commun. (2000) 1061;
(c) Y.-C. Jiang, Y.-C. Lai, S.-L. Wang, K.-H. Lii, Inorg. Chem. 40 (2001) 5320;
(d) L.-H. Huang, H.-M. Kao, K.-H. Lii, Inorg. Chem. 41 (2002) 2936;
(e) L.-I. Hung, S.-L. Wang, H.-M. Kao, K.-H. Lii, Inorg. Chem. 41 (2002) 3929;
(f) W.-K. Chang, R.-K. Chiang, Y.-C. Jiang, S.-L. Wang, S.-F. Lee, K.-H. Lii, Inorg. Chem. 43 (2004) 2564;
(g) Z. Shi, S. Feng, S. Gao, L. Zhang, G. Yang, J. Hua, Angew. Chem. Int. Ed. 39 (2000) 2325.
[3] W.-J. Chang, C.-Y. Chen, K.-H. Lii, J. Solid State Chem. 172 (2003) 6.
[4] W.-J. Chang, P.-C. Chang, H.-M. Kao, K.-H. Lii, J. Solid State Chem. 178 (2005) 3709.
[5] (a) Y. Zhang, R.C. Haushalter, J. Zubieta, Inorg. Chim. Acta 260 (1997) 105;
(b) R. Finn, J. Zubieta, Chem. Commun. (2000) 1321;
(c) Z. Shi, S. Feng, L. Zhang, G. Yang, J. Hua, Chem. Mater. 12 (2000) 2930;
(d) W. Yang, C. Lu, Inorg. Chem. 41 (2002) 5638;
(e) Y. Lu, E. Wang, M. Yuan, G. Luan, Y. Li, H. Zhang, C. Hu, Y. Yao, Y. Qin, Y. Chen, J. Chem. Soc. Dalton Trans. 4 (2002) 3029;
(f) Z.-E. Lin, Y.-Q. Sun, J. Zhang, Q.-H. Wei, G.-Y. Yang, J. Mater. Chem. 13 (2003) 447;
(g) Z.-E. Lin, J. Zhang, S.-T. Zheng, G.-Y. Yang, Inorg. Chem. Commun. 6 (2003) 1035;
(h) Z.-E. Lin, J. Zhang, Y.-Q. Sun, G.-Y. Yang, Inorg. Chem. 43 (2004) 797;
(i) H. Meng, G. Li, Y. Liu, L. Liu, Y. Cui, W. Pang, J. Solid State Chem. 177 (2004) 4459;
(j) Z.-E. Lin, J. Zhang, S.-T. Zheng, G.-Y. Yang, Solid State Sci. 7 (2005) 319.
[6] G.M. Sheldrick, SADABS, Program for Siemens Area Detector Absorption Corrections, University of Göttingen, Germany, 1997.
[7] I.D. Brown, D. Altermatt, Acta Crystallogr. B 41 (1985) 244.
[8] G.M. Sheldrick, SHELXTL Programs, Version 5.1, Bruker AXS GmbH, Karlsruhe, Germany, 1998.
[9] O. Kahn, Molecular Magnetism, VCH, New York, 1993.
[10] C.-Y. Chen, P.P. Chu, K.-H. Lii, Chem. Commun. 4 (1999) 1473.